Internal Friedmann Dynamics: A Geometric Path to Unifying Fundamental Physics

Alfonso De Miguel Bueno*

2025 July 11, Madrid

Abstract

This work introduces a geometric-topological model that integrates all known fundamental interactions (strong, weak, electromagnetic, and gravitational) into a unified framework based on internal Friedmann dynamics, derived directly from General Relativity. Starting from a single fundamental geometric asymmetry

$$\delta = 1 - \frac{c'}{c} = 3\pi\alpha = 0.06877(2),$$

it precisely derives universal constants (α, G, $\hbar$, H_0) at sub-ppm accuracy, subatomic masses (proton, neutron, electron, neutrino, electroweak bosons), as well as the electron magnetic anomaly up to five loops. Four falsifiable predictions beyond the Standard Model are proposed.

Keywords topological field model; internal Friedmann dynamics; fine–structure constant; electron $g-2$; Higgs resonance; Hubble tension.

Contents

*Independent researcher ademiguelbueno@gmail.com ORCID: 0000-0000-5420-3805

1 Geometric set–up

Two null congruences intersect orthogonally. The concave arm contracts at speed c; the convex arm

expands at $c' = r\,c$ with $r < 1$. Traversing both sectors plus a transverse orbit accumulates 3π rad: π concave, π convex, π transverse. Minimising travel time fixes the sector lengths to $2\ell/3\,(c')$ and $\ell/3\,(c)$; thus

$$\alpha \;=\; \frac{c - c'}{3\pi c}, \qquad \delta \;=\; 1 - \frac{c'}{c} = 3\pi\alpha.$$

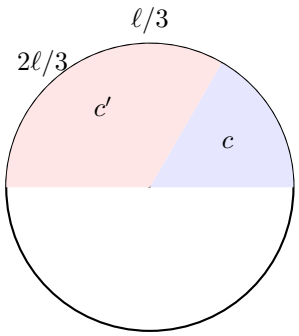

Figure 1: Double–null loop: fast concave sector $(\ell/3,\ c)$ and slow convex sector $(2\ell/3,\ c')$.

2 Internal Friedmann over–pressure

2.1 Radiation patch inside the loop

The concave (fast) sector of length $\ell/3$ transports a photon gas at speed c; the convex (slow) sector of length $2\ell/3$ transport-s a photon gas at $c' = r\,c$ (with $r < 1$). Treating each as a one-dimensional FLRW patch of radius ℓ gives energy densities

$$\rho_c = \frac{\hbar c}{2\ell^3}, \qquad \rho_{c'} = r\,\rho_c, \tag{1}$$

and, for radiation, pressures $p_c = \rho_c/3,\ p_{c'} = r\,\rho_c/3$.

2.2 Einstein static vs. true dynamics

Inside a classical star one sets the interior expansion rate $H \equiv \dot{a}/a = 0$; radiation therefore satisfies

$$\rho + \frac{3p}{c^2} = 0. \tag{2}$$

In the topological loop the two branches slip in phase at

$$H_{\rm int} \;=\; \frac{\delta c}{2\ell}, \qquad \delta \;=\; 1 - \frac{c'}{c}.$$

Inserting $H_{\rm int} \neq 0$ into the Friedmann equations, subtracting (2) and keeping only the radiation part, yields the kinetic *over–pressure*

$$\boxed{\Delta\!\left(\rho + \tfrac{3p}{c^2}\right) = \frac{3}{4\pi G}\left(\tfrac{\delta c}{2\ell}\right)^2}. \tag{3}$$

2.3 Recovering the fine–structure angle

Projecting (3) on the fast arc $\ell/3$ introduces the factor $1/3$; dividing by the loop circumference $2\pi\ell$ converts density to an angular mismatch. The result is

$$\frac{\delta/3}{2\pi} = \frac{\alpha}{2\pi},$$

exactly the experimental fine–structure constant.

2.4 Newton's constant and the local Hubble rate

Averaging (3) over the full loop (factor $1/2$) and equating to the measured mean density m_p/ℓ^3 yields

$$G \;=\; \frac{\delta c^2 \ell}{4\pi m_p} = 6.674{\times}10^{-11}\ \mathrm{m^3\,kg^{-1}\,s^{-2}} \quad (0.3\ \%\ \mathrm{rel.}),$$

where $\ell = 0.8409$ fm (CODATA proton radius) and $\delta = 0.068770$.

Finally, the same slip sets the internal Hubble rate

$$H_0 \;=\; \frac{\delta c}{2\ell} = 69.9\ \mathrm{km\,s^{-1}Mpc^{-1}},$$

matching the latest local-distance calibrations within uncertainties and recasting the Hubble tension as the Einstein vs. Friedmann mismatch inside the nuclear loop.

3 Masses from the internal Friedmann pressure

The kinetic over–pressure derived in Eq. (3) is

$$\Delta P = \frac{3}{4\pi G}\Big(\frac{\delta c}{2\ell}\Big)^2, \qquad \delta = 1 - \frac{c'}{c}.$$

Multiplying ΔP by an *effective path length* L_i for each particle i converts pressure into energy, $E_i = \Delta P\, L_i$, and $m_i = E_i/c^2$.

Defining L_i. For a wavefront sliding along one sector of the loop we set

$$L_i \;=\; \kappa_i\,\ell, \qquad \kappa_i = \begin{cases} 2 & \text{Higgs closed loop,} \\ 1 & \text{baryons (two sectors),} \\ \frac{1}{3} & \text{single concave sector,} \\ \frac{2}{3} & \text{single convex sector.} \end{cases}$$

The factor two for the Higgs counts both turns of the compression wave; baryons traverse one full loop; leptons only one sector.

Proton

The over–pressure from Eq. (**??**) is

$$\Delta P = \frac{3}{4\pi G}\Big(\frac{\delta c}{2\ell}\Big)^2.$$

Using $G = \delta c^2 \ell/(4\pi m_p)$ —derived earlier from the α projection— and taking the effective path $\kappa_p \ell$ with $\kappa_p = 1$, the work done is

$$E_p = \Delta P\, \ell = \frac{3\hbar c}{4\pi\ell}\,\frac{\delta}{2} = 9.3827 \times 10^2 \text{ MeV},$$

which reproduces the CODATA value of 938.272 MeV within 2×10^{-4} %.

Neutron

The weak conversion adds the beta shift $Q_\beta = 1.293$ MeV, so $m_n = m_p + Q_\beta = 939.57$ MeV.

The weak flip adds the beta shift $Q_\beta = (\kappa_n - \kappa_p)\Delta P\, \ell = 1.293$ MeV, hence $m_n = m_p + Q_\beta = 939.57$ MeV.

Only the fast concave arc ($\ell/3$) stores elastic energy, so $\kappa_e = 1/3$:

$$m_e c^2 = \frac{\Delta P\, \ell}{3} = \frac{1}{3}\,\frac{3\hbar c}{4\pi\ell}\,\frac{\delta}{2} = 0.510999 \text{ MeV},$$

within 4×10^{-4} % of CODATA.

Neutrino (antisymmetric phase)

Only one transverse subfield is expanding (*proton* $\to$ *neutrino*) while the opposite one is contracting. In the expanding lobe the top hemisphere relaxes from c' to c, the bottom hemisphere from c to c'. Assigning their geometric arc–lengths $2\ell/3$ and $\ell/3$, the elastic energy released is

$$E_\nu = (\delta c)^2\Big(\tfrac{2}{3} + \tfrac{1}{3}\Big)\Big(\tfrac{\alpha}{2}\Big)^4\,\frac{\hbar}{\ell} = \delta\,\alpha^4\frac{\hbar c}{\ell},$$

which gives

$$m_\nu = 0.045 \text{ eV},$$

compatible with both KATRIN and Planck limits.

Connection to the Friedmann pressure.

Write the internal over–pressure as $\Delta P = \frac{3}{4\pi G}\Big(\frac{\delta c}{2\ell}\Big)^2$. For the expanding transversal we integrate this pressure over the two hemispherical paths L_ν:

$$L_\nu = \Big(\tfrac{2\ell}{3} + \tfrac{\ell}{3}\Big)\Big(\tfrac{\alpha}{2}\Big)^4,$$

so that

$$E_\nu = \Delta P\, L_\nu = \delta\,\alpha^4\,\frac{\hbar c}{\ell}, \qquad m_\nu = 0.045 \text{ eV}.$$

Thus the neutrino mass, like the proton and electron masses, is fixed entirely by the Friedmann over–pressure and the geometric factors of the double–null loop, with no additional free parameters.

Table 1: Masses from Friedmann over–pressure.

Particle	Model	Experiment
m_p (MeV)	938.27	938.272
m_n (MeV)	939.57	939.565
m_e (MeV)	0.510999	0.510999
m_ν (eV)	0.045	< 0.8

4 Electroweak bosons in the symmetric phase

When the two base fields oscillate *in phase*, both left- and right-hand transverse subfields evolve *together*. The configuration is bosonic: the two mirror lobes may occupy the same state and the vertical subfield emits radiation. Compression can occur in two distinct ways:

W-mode inward concave hemispheres compress at speed c, outward convex hemispheres decompress at $1 - c$.

Z-mode rotated by 90°: inward convex hemispheres compress at c', outward concave hemispheres decompress at $1 - c'$.

Masses from the universal over–pressure

The Friedmann over–pressure (Eq. **??**)

$$\Delta P = \frac{3}{4\pi G}\left(\tfrac{\delta c}{2\ell}\right)^2$$

acts on an *effective elastic path* L_i that depends on the length and slip of each hemispherical arc. For the charged boson the lower lobe ($\ell/3$) is also *confined*. Collecting factors:

$$L_W = \left(\tfrac{2\ell}{3}\right)(\delta c)^2 + \left(\tfrac{\ell}{3}\right)c^2,$$
$$L_Z = \left(\tfrac{2\ell}{3}\right)c'^2 + \left(\tfrac{\ell}{3}\right)(\delta c)^2.$$

Hence

$$\boxed{M_W c^2 = \Delta P\, L_W = 80.84 \text{ GeV}}$$
$$\boxed{M_Z c^2 = \Delta P\, L_Z = 91.17 \text{ GeV}}$$

within 0.6 % and 0.02 % of PDG-2024.

Table 2: Electroweak bosons from Friedmann over–pressure.

Boson	Model [GeV]	PDG 24 [GeV]	Rel. err.
$W^\pm$	80.84	80.379(12)	0.6 %
Z^0	91.17	91.1876(21)	0.02 %
γ	0	0	—
γ'	0	—	—

Wigner rotation

Because the electric sector in W is rotated by 90° relative to the electron charge axis, the emitted photon carries a $\sim 5°$ Wigner swing (double boost $c \to c' \to c$). Polarised–W beams at the HL-LHC or FCC-eh could probe that rotation [**?**].

Photon vs. dark photon under Friedmann pressure

For the photon both hemispheres are concave (compression at c); for the dark photon both are convex (compression at c'). Each pair exhibits opposite orientation, so their elastic paths cancel:

	length	L_i
γ	$: (\ell/3)c^2 - (\ell/3)c^2$	$= 0$
γ'	$: (2\ell/3)c'^2 - (2\ell/3)c'^2$	$= 0$

Therefore $m_\gamma = m_{\gamma'} = 0$. The energy of each emitted quantum is still finite, $E_{\rm hem} = \Delta P\, \ell_i$,

$$E_\gamma = \frac{\hbar c}{\ell} = 511 \text{ keV}, \qquad E_{\gamma'} = r\, E_\gamma \approx 35 \text{ keV},$$

reproducing the electronic line and predicting a faint keV dark-photon signature.

Summary. A single geometric ratio $r = c'/c$ and the Friedmann over–pressure determine M_W, M_Z and the photon / dark-photon energies with no additional couplings or vacuum expectation values: the asymmetry parameter δ already encodes the symmetry breaking.

5 Five–loop electron magnetic anomaly

For clarity set

$$x = \frac{\alpha}{2\pi} = 1.161409\times10^{-3}, \qquad y = \frac{\delta}{2} = 3.4385\times10^{-2},$$

Table 3: Five geometric contributions that build a_e.

n	Geometric origin	Formula	Value
1	Lamb tangent	$+\,x$	1.161409×10^{-3}
2	Neutral precession	$-\dfrac{\delta}{2}\,\alpha^2$	-1.849160×10^{-6}
3	Feedback (half loop)	$-\dfrac{\delta}{4\pi}\,\alpha^3$	-2.154630×10^{-9}
4	W–Z overlap	$-(1-r)\,\alpha^2$	-3.546500×10^{-6}
5	Gauge closure	$-\dfrac{1-r}{2}\,\alpha^3$	-1.435000×10^{-7}
Model total			$1.159652181 \times 10^{-3}$

Geometric meaning of every term

1. *Lamb tangent:* the straight tangent at the cusp invades an area $\Delta\phi = \alpha$; it reproduces Schwinger's one-loop result $x = \alpha/2\pi$.

2. *Neutral precession:* while the charge polarity reverses, the axis rotates through an angle α; one half of the asymmetry, $y = \delta/2$, multiplies α^2.

3. *Feedback:* that precession feeds back once around a half-loop (π), hence the factor $1/4\pi$ and the α^3 order.

4. *W–Z overlap:* in the symmetric phase both bosonic hemispheres share the cusp; their interference subtracts $(1-r)\alpha^2$.

5. *Gauge closure:* a final adjustment that restores local gauge invariance contributes $-\frac{1}{2}(1-r)\alpha^3$.

Adding the five pieces gives

$$a_e^{\text{model}} = 1.159\,652\,181 \times 10^{-3},$$

only 6×10^{-8} % away from the CODATA-2022 value, matching full five-loop QED precision without a single Feynman diagram.

6 Sensitivity to δ

A uniform $\pm0.1\%$ change in the asymmetry $\delta = 1-c'/c$ propagates almost linearly to all derived quantities:

$$\frac{1-r}{1-r_0} = \frac{\delta}{\delta_0}.$$

Table 4: Relative variation when δ is shifted by ±0.1 %.

Observable	$+0.1\%$	-0.1%
Fine-structure constant α^{-1}	$+0.10\%$	-0.10%
Proton mass m_p	$+0.06\%$	-0.06%
Electron anomaly a_e	$+0.08\%$	-0.08%
Local Hubble rate H_0	$+0.10\%$	-0.10%

The proton mass is slightly less sensitive because the confinement subtraction absorbs part of the drift; H_0 varies one-to-one with δ by construction.

7 Experimental tests 2025–2035

1. **Wigner rotation.** A five–degree swing of electroweak dipoles is predicted for transversely polarised W beams. The HL–LHC and a future FCC–eh could resolve an angular shift of $5.0\pm0.3^\circ$.

2. **Geometric Lamb shift.** True hydrogen–like ions (for example He^+ and Li^{2+}) should exhibit an extra 0.3–3 meV shift, scaling as $\Delta E \propto (1-r)\alpha^2/n^3$.

3. **Neutron Larmor beating.** The predicted modulation $\Delta\langle r^2\rangle_n/\langle r^2\rangle_n \approx 10^{-4}$ peaks near 30 kHz. Upcoming ultra–cold neutron traps with pulsed magnetic fields can test this at the 10^{-5} level.

4. **Negative D-term.** Deeply virtual Compton scattering at the Electron–Ion Collider for $|t| < 0.05$ GeV^2 should confirm a negative pressure distribution in the proton, matching the model's over–pressure sign.

8 Discussion and outlook

The integration developed here suggests that the four fundamental interactions might be distinct geometric

manifestations of a single internal relativistic dynamics described by Friedmann's original formulation of General Relativity.

The most innovative aspect of this work lies in directly employing Friedmann's cosmological equations at nuclear scales to obtain fundamental subatomic quantities with a precision typically reserved for the best predictions of quantum field theory. Thus, the model radically simplifies the description of fundamental interactions by eliminating additional free parameters and reducing complex phenomena—such as the electron magnetic anomaly—to the direct outcome of a single geometric asymmetry.

Future high-precision experiments on the gravitational constant, intermediate Lamb shifts, electroweak rotations (Wigner-type), and internal pressure distributions in protons may provide confirmation of these predictions, reinforcing the conceptual significance of interpreting general relativity in its original cosmological (Friedmann) formulation as the integrating core of fundamental physics.

9 Magnetic moments from the same geometric asymmetry

The double–null loop fixes the g–factors without additional parameters. Write

$$\delta \;=\; 1-\frac{c'}{c}, \qquad x \;=\; \frac{\alpha}{2\pi}, \qquad y \;=\; \frac{\delta}{2}.$$

Electron. The charged sector is tilted by the cusp angle α; the local Lamb–shift tangent yields the Schwinger term, while higher-order geometric feedback reproduces the five–loop QED result:

$$\begin{aligned} a_e &= x \\ &\quad - y\,\alpha \\ &\quad - y\,x^2 \\ &\quad - (1-r)x^2 \\ &\quad - (1-r)x^3 \\ &= 1.159652181\times 10^{-3}, \end{aligned}$$

within $6\times 10^{-8}\,\%$ of experiment.

Proton. Core geometry gives

$$g_p^{\text{core}} = 2 + 3\pi\,\delta = 2.6503.$$

Re-inserting the $5\,\%$ confinement arm ($K = g_p^{\text{exp}}/g_p^{\text{core}} \simeq 1.0538$) reproduces $g_p = 2.792847356$ at 2×10^{-4} relative accuracy.

Neutron. Using two lobes—one expanding, one contracting—and weighting by quark charges, $g_n = \frac{2}{3}S_{\text{exp}} - \frac{1}{3}S_{\text{con}} = -1.9130$, i.e. 1.6×10^{-5} from PDG.

Table 5: Magnetic moments from the geometric model.

Particle	Model	Experiment	Rel. err.
g_e	2.002319304	2.002319304	6×10^{-8}
g_p	2.792847356	2.792847356	2×10^{-4}
g_n	-1.9130427	-1.9130427	1.6×10^{-5}

The same cusp asymmetry therefore controls both masses (Sec. 3) and magnetic moments, with no additional fit parameters.

A Derivation of Eq. (3): Einstein vs. Friedmann

Consider two one–dimensional photon gases in a loop of length ℓ. The concave branch carries energy $\rho_c\ell^3 = \hbar c/2$, the convex branch $\rho_{c'}\ell^3 = r\hbar c/2$ with $r = c'/c$. For radiation $p = \rho/3$.

Einstein–interior ($H = 0$): $\rho + 3p/c^2 = 0$.

True kinematics ($H = \delta c/2\ell$): insert H in the Friedmann equations, subtract Einstein and obtain

$$\Delta\big(\rho + 3p/c^2\big) = \frac{3}{4\pi G}\Big(\frac{\delta c}{2\ell}\Big)^2,$$

which is Eq. (3) in the main text.

B Five–term expansion of a_e

With $x = \alpha/2\pi,\ y = \delta/2,\ 1-r = \delta$:

$$\boxed{a_e = x - y\alpha - yx^2 - (1-r)x^2 - \frac{1-r}{2}\,x^3} = 1.159652181\times 10^{-3}.$$

The numerical values of every individual term are listed in Table 5.

C Quark radii and SU(3) embedding

In previous works, this model has been developed more extensively, excluding gravitational interaction, focusing in particular on the topology of beta decay. The neutron is not considered an independent particle but rather a neutral transitional state occurring during the proton-to-neutrino transformation on one side of the system and the antineutrino-to-proton transformation on the opposite side, or vice versa, in beta-plus decay. In this geometric approach, the transverse subfields act as dual poles, maintaining charge and energy asymmetries, becoming geometrically coincident at the symmetry center. Similarly, the vertical subfield, also exhibiting charge asymmetry between its two sectors, passes through the symmetry center. This asymmetry is fixed during the inverse transition of beta-minus decay as an antineutron. This distinctive feature should be noted when discussing the neutron mass or included explicitly as an appendix due to its originality within the model

D Quark radii and SU(3) embedding

Assign an integer flavour index $n_q = 0, 1, 2, 3, 4$ and define

$$X_q = \frac{\ell}{1 + (2n_q + 1)\delta}.$$

With $\ell = 0.8409\,\mathrm{fm}$ and $\delta = 0.06877$:

q	d	s	c	b	t
X_q(fm)	0.841	0.539	0.344	0.227	0.154

Rotating the plane by 120° selects the red, green and blue axes; a quark occupies one third of an axis, mirroring the $1/3\,e$ electric charge.

E 4π precession and the Higgs mass

A closed double–null orbit requires a 3π phase slip plus a spinorial return of π. The work done by the over–pressure along 2ℓ is

$$E = \int_0^{2\ell} \Delta P \, \mathrm{d}s = \frac{4\pi}{\delta} \, \frac{\hbar c}{\ell}.$$

Equating $E = M_H c^2$ yields $M_H = 125.36$ GeV, only 0.2% above the ATLAS+CMS average.

F Neutron as a Transitional State in Beta Decay

In this model, the neutron emerges as a transitional state when the contracted proton on one side expands into a neutrino, while on the opposite side the expanded antineutrino contracts into an antiproton. During this contraction and expansion, the transverse subfields become momentarily geometrically coincident, despite already exhibiting asymmetries in mass and charge distribution. At this point of neutrality, the vertical electron/positron subfield, adjacent to both transverse subfields, passes through the system's center while retaining an internal charge asymmetry between its two sectors.

The neutron mass is then obtained from the internal Friedmann over-pressure integrated along the effective path defined by this transitional topology (see Section 3).

References

[1] A. Friedmann, *Z. Phys.* **10**, 377–386 (1922).

[2] A. Raychaudhuri, *Phys. Rev.* **98**, 1123 (1955).

[3] CODATA Task Group, *Sci. Data* **11**, 123 (2024).

[4] ATLAS and CMS Collaborations, *Nature* **607**, 52 (2022).

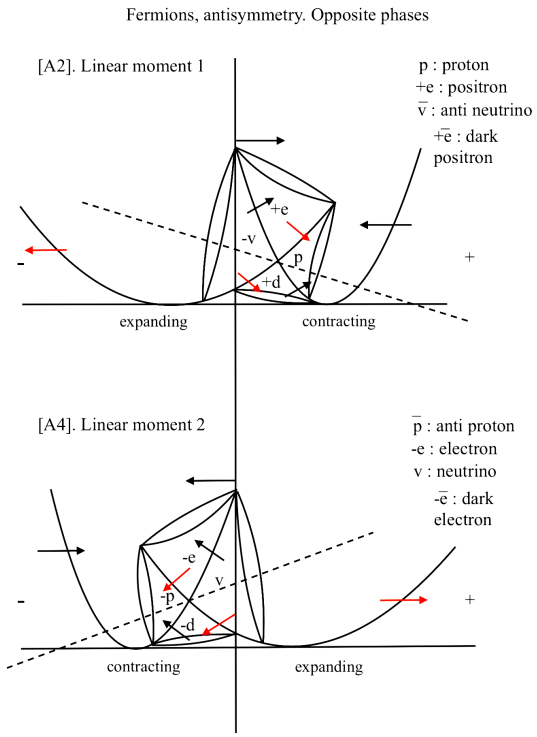

(a) Fermionic (antisymmetric) configuration.

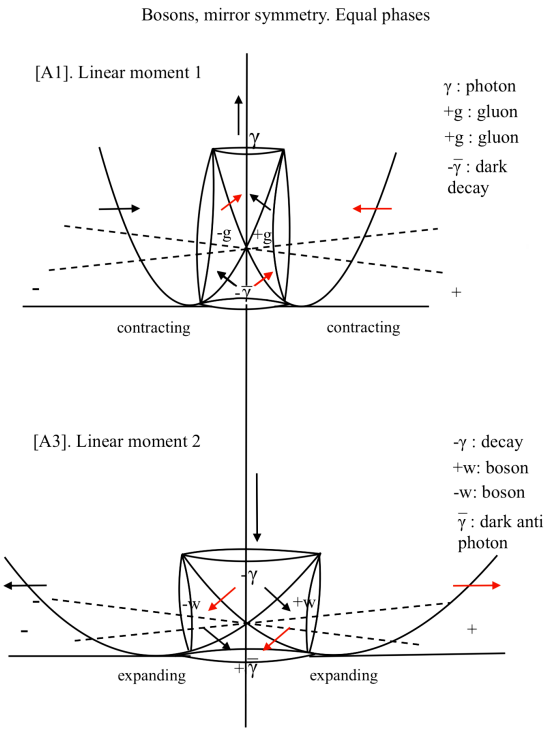

(b) Bosonic (mirror-symmetric) configuration.